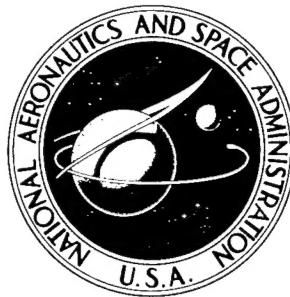


NASA (TECHNICAL NOTE)



NASA TN D-3426

NASA TN D-3426

AMPTIAC

DISTRIBUTION STATEMENT A
Approved for Public Release
Distribution Unlimited

ACCELERATED CAVITATION DAMAGE OF STEELS AND SUPERALLOYS IN LIQUID METALS

by Stanley G. Young and James R. Johnston

NASA
Lewis Research Center
Cleveland, Ohio

20020319 155

ACCELERATED CAVITATION DAMAGE OF STEELS ⁴
AND SUPERALLOYS IN LIQUID METALS)

By Stanley G. Young ⁵ and James R. Johnston ⁶

^{NASA}
Lewis Research Center ⁵
Cleveland, Ohio ⁶

NATIONAL AERONAUTICS AND SPACE ADMINISTRATION

For sale by the Clearinghouse for Federal Scientific and Technical Information
Springfield, Virginia 22151 - Price \$2.00

*start extract
p. 12*

ACCELERATED CAVITATION DAMAGE OF STEELS AND SUPERALLOYS IN LIQUID METALS

by Stanley G. Young and James R. Johnston

Lewis Research Center

SUMMARY

An investigation was conducted to study cavitation damage in liquid metal environments of materials under consideration for components of liquid metal power conversion systems. The materials investigated included AISI-316 and 318 stainless steels, Sicromo 9M, Inconel 600, A-286, Hastelloy X, L-605, René-41, and Stellite 6B. A magnetostrictive apparatus was used to perform accelerated cavitation damage tests with liquid sodium at 800° F and mercury at 300° F. Cavitation damage determined by volume loss and surface roughness measurements was used to rank the various materials, and to compare the effects of the different fluids on the degree of damage sustained. Metallographic studies were made to determine the nature of the early stages of cavitation damage. *Lead*

The materials tested in both sodium and mercury ranked in the same order of resistance to cavitation damage, but the degree of damage to all materials was consistently greater when tested in mercury. The most resistant material by far was Stellite 6B; the least resistant material was annealed Sicromo 9M. Surface roughness measurements were found to provide the same ranking of materials as that provided by conventional volume loss measurements. Visual observation of sodium pump impeller blades of three materials operated under cavitating conditions for 250 hours indicated the same ranking of the materials with respect to resistance to cavitation damage that was determined from the accelerated cavitation tests.

INTRODUCTION

In advanced space power conversion systems that use liquid metals for the heat-transfer medium, cavitation damage to both rotating and stationary components of the system may be expected. Damage can occur in pumps and in stationary sections of the

system where local pressure fluctuations occur in the fluid. Components tested for relatively short times in liquid metal loops have shown damage in the form of pitting and surface erosion (refs. 1 to 3). Damage has also been observed in the turbine component of liquid metal systems when the vapor quality was less than 100 percent (ref. 4). It has been reported that materials which resist cavitation attack are also resistant to liquid impingement (ref. 5). Because proposed space power systems must function for times in excess of 10 000 hours, it is important to establish the resistance to cavitation damage of materials that may be used in various components of such systems.

Extensive research has been conducted to study the mechanism of cavitation and cavitation damage of materials in water (refs. 6 to 15). Cavities form in moving fluids where local pressures fall below the vapor pressure of the fluid. When these cavities are swept into regions of higher pressure, they collapse with high velocity. If the collapse is on a metal surface, localized high pressures that are transmitted to the metal can cause severe damage. Although much of this damage is of a mechanical nature, it has also been shown that corrosion can be a contributing factor (refs. 7, 11, and 15). Conventionally used engineering properties such as hardness, tensile and yield strengths, fatigue limit, and corrosion resistance have all been considered as means of ranking materials with respect to resistance to cavitation damage. None of these properties individually provides a satisfactory criterion for rating materials; however, recent work indicates that strain energy may correlate with the intensity of cavitation damage for a number of materials (ref. 16).

In order to study a great number of materials in relatively short times, various accelerated test methods for producing cavitation damage have been devised. These include the rotating disk method (ref. 13), venturi systems (ref. 17), and magnetostrictive systems (ref. 15). All of these methods have been adapted for use in liquid metal environments (refs. 14, 18, and 19). Of these methods the magnetostrictive apparatus was selected for this investigation because it afforded a relatively low cost and versatile means of producing highly accelerated cavitation damage. With this facility various materials currently under consideration for use in components of liquid metal space power conversion systems were investigated in both sodium and mercury for resistance to cavitation damage. The purposes of the investigation were as follows: to rank these materials according to their resistance to cavitation damage, to determine the nature of the early stages of cavitation damage by metallographic studies, and to correlate accelerated cavitation test data with cavitation damage sustained in actual pump operation in liquid metal loops.

A number of iron-, nickel-, and cobalt-base alloys were investigated in sodium at 800° F and in mercury at 300° F under argon at 1 atmosphere. The vapor pressures of these two fluids were nearly equal at these temperatures. Cavitation damage was inves-

tigated by obtaining volume loss and surface roughness measurements and by metallographic studies.

MATERIALS, APPARATUS, AND PROCEDURE

Materials

Specimens. - The materials tested for resistance to cavitation damage were the iron-base alloys, Sicromo 9M, A-286, and AISI 316 and 318 stainless steels; the nickel-base alloys, Inconel 600, Hastelloy X, and René 41; and the cobalt-base alloys, L-605 and Stellite 6B. The nominal chemical composition of each alloy is listed in table I. The heat treatments employed and the densities of these alloys are listed in table II. Specimen material was obtained in the form of 5/8- or 3/4-inch bar stock.

Test fluids. - Reactor-grade sodium (99.95 percent pure) and triple-distilled mercury were used as the test fluids. Chemical analyses indicated an initial oxygen level of 10 to 41 parts per million for the sodium. The mercury had a 0.2 part per million total impurity content. Sodium was supplied in 3-pound-capacity stainless-steel containers, and mercury was supplied in conventional polyethylene containers.

Apparatus

The facility used is shown in figure 1. The photograph shows the vacuum dry box and associated electronics and control equipment. A schematic diagram of the test apparatus is shown in figure 2, and details of the transducer-specimen assembly are shown in figure 3. Figure 2 illustrates the dry box arrangement, magnetostrictive transducer assembly, and separately sealed liquid metal test chamber. The dry box and test chamber were designed to be evacuated to a pressure of approximately 10^{-3} torr (1μ) and were backfilled with high-purity argon containing less than 1 part per million oxygen and 6 parts per million water vapor. Glove ports were provided on the dry box to enable the operator to change specimens and to work within the argon atmosphere.

The transducer was a commercial unit, modified for use within the vacuum dry box. The specimen was attached to the end of a resonant system consisting of the transducer, an amplifying exponential horn, and an extension-rod specimen holder. The horn served as a displacement amplifier and provided a convenient attachment for a nodal flange vapor seal (fig. 2). A 1-wavelength extension rod (approx 8 in. long) was chosen to permit location of the hot zone of the furnace at a convenient distance from the transducer assembly. The amplitude and frequency of vibration were detected by a magnetic pickup.

This signal was sent to an oscilloscope and to an automatic feedback system that maintained a constant amplitude of vibration irrespective of variations in resonant frequency induced by temperature changes. The output of the magnetic pickup was calibrated against optical measurements of amplitude made with a 200-power microscope equipped with a filar eyepiece.

When the transducer assembly was lowered into position, the sleeve attached to the nodal flange on the amplifying horn sealed the liquid metal test chamber from the dry box. The test chamber pressure was regulated through a separate argon line. The liquid metal was heated by a resistance furnace, and the bath temperature was measured with a stainless-steel-clad Chromel-Alumel immersion thermocouple. The liquid metal test chamber also was made of stainless steel.

Test Conditions

During this investigation an argon pressure of 1 atmosphere was maintained above the liquid metal. Sodium tests were run at $800^{\circ}\pm 10^{\circ}$ F, and mercury tests at $300^{\circ}\pm 30^{\circ}$ F. At these temperatures the vapor pressures of both fluids were less than 0.1 pound per square inch. The frequency of vibration of the test specimens was nominally 25 000 cps, and the peak-to-peak displacement amplitude was 0.00175 (± 0.00005) inch. Specimens were immersed to a depth of approximately 1/8 inch below the surface of the liquid metal.

Test Procedure

The type of specimen used is shown in figure 4. The test surface of each specimen was metallographically polished and then marked with a series of microhardness impressions to delineate specific areas for metallographic examination.

Specimens were first cleaned with acetone and then with alcohol and subsequently dried in warm air. The marked areas of the specimens were photographed, and the specimens were weighed on an analytical balance to a precision of ± 0.05 milligram. Specimens were subjected to cavitation damage by vibration for varying intervals. After each period of operation, the specimens were removed from the test facility, cleaned, and weighed; then photomicrographs and macrographs were taken. Weight loss measurements were divided by density to obtain volume loss. Surface roughness traces of the central portions of the specimens were obtained with a linear profiler having a diamond stylus of 0.0005-inch radius and a cone angle of 51.5° . Maximum total test duration for any material was 4 hours.

Different cleaning procedures were required for specimens that were removed from each of the two fluids. After testing in sodium, specimens were washed first in methyl alcohol; then, when all sodium was removed, specimens were rinsed in water and dried. After mercury tests, the specimens were ultrasonically vibrated above the mercury bath to drive off any excess mercury. Specimens were then placed under vacuum at 500° F for several hours to remove any mercury that might have remained on the specimen.

CAVITATION DAMAGE RESULTS

Volume Loss

Cavitation damage is expressed as volume loss for nine materials in sodium and five materials in mercury in figures 5(a) and (b), respectively. Volume loss data for all materials are also summarized in table III. The materials tested in sodium were ranked in order of increasing damage as follows: Stellite 6B, René 41, L-605, Hastelloy X, A-286, Inconel 600, AISI 318 stainless steel, AISI 316 stainless steel, and annealed Sicromo 9M.

A wide range of damage was observed for the various materials. For example, after 4 hours the most resistant material, Stellite 6B, exhibited approximately 15 percent of the damage sustained by L-605, another of the more resistant alloys, but only approximately 1 percent of the damage sustained by annealed Sicromo 9M, the most heavily damaged material.

The materials tested in mercury were ranked in order of increasing damage as follows: Stellite 6B, hardened Sicromo 9M, L-605, Hastelloy X, and annealed Sicromo 9M. Again a wide range in the degree of damage was observed. For example, after 4 hours, the most resistant material, Stellite 6B, showed approximately 16 percent of the damage sustained by L-605. After 1 hour, the damage to Stellite 6B was approximately 2 percent that of annealed Sicromo 9M.

Annealed Sicromo 9M, with an original Rockwell hardness of B-80, was heat treated to a hardness of Rockwell C-40. The hardened alloy at 1 hour showed only about 6 percent of the damage sustained by this alloy in the annealed condition. In this particular instance increasing the hardness, substantially increased resistance to cavitation damage.

The materials tested in both sodium and mercury ranked in the same order of resistance to cavitation damage; however, the cavitation damage experienced by all materials in mercury at 300° F was two to seven times greater on the basis of total volume loss than the damage experienced by the same materials in sodium at 800° F.

Volume Loss Rate

Curves of volume loss rate for all the materials investigated are shown in figure 6. These curves represent the changes in the volume loss with respect to time as determined from the volume loss curves faired through the actual data. Portions of the rate curves for some materials are dotted because the exact shape of the volume loss curves is uncertain. The rate curves generally suggest that there is an initial low damage rate, then a steadily increasing rate until a peak damage rate is reached, and finally a decreasing rate until a steady-state condition is achieved. This has also been reported by other investigators (ref. 20). When the materials are compared on the basis of their steady-state damage rate, they rank in the same order with respect to resistance to damage as when compared on the basis of total volume loss. Steady-state volume loss rates are listed in table III.

Surface Roughness Measurements

Because cavitation damage is usually measured quantitatively in terms of weight or volume loss, it is sometimes difficult because of limited accessibility to accurately measure the damage to system components such as tubing or impellers. If a correlation could be shown between volume loss and surface roughness measurements, it is conceivable that the latter might be used to measure quantitatively the cavitation damage to these components.

Cavitation damage was measured in terms of surface roughness for all the materials tested in mercury and four of the materials tested in sodium. These measurements are also summarized in table III. Table IV provides a typical example of surface roughness as compared with volume loss measurements for L-605 after testing in mercury at 300° F. The surface traces shown in the table depict the surface contour, magnified vertically 1000 times. The arithmetic average surface roughness values in microinches are also presented.

A comparison of the arithmetic average surface roughness with volume loss as a function of test time is shown after testing in sodium and in mercury in figures 7(a) and (b), respectively. The materials are ranked in the same order on the basis of both surface roughness and volume loss. Surface roughness measurements are extremely sensitive, and a clear distinction among the materials as to relative cavitation damage resistance can be made by this method during the early stages of damage even though very little volume loss has occurred.

A cross plot between the volume loss and surface roughness measurements for given

times (fig. 8) indicates that, in the case of specimens damaged in sodium, the surface roughness tends to approach constant values with increasing volume loss. These constant values of surface roughness correspond to the steady-state volume loss rates illustrated in figure 6(a).

In the case of specimens damaged in mercury, however, the surface roughness, in general, tends to increase with increasing volume loss and does not appear to approach constant values as might be expected from the appearance of the volume loss rate curves for mercury (fig. 6(b)). These results suggest that the mechanism of cavitation attack by mercury may be quite different from that by sodium. Additional evidence to this effect will be shown in the next section. Briefly, damage to materials in sodium is evidenced by a general attrition of the surface, which is shown by the relatively fine-textured surface that erodes uniformly. Damage due to cavitation in mercury is evidenced by the formation and continual deepening of wide craters.

Metallography

Macrographs were taken of all materials after various exposure times. The damaged surfaces of one of the least and one of the most cavitation-resistant materials are illustrated after different exposure times to sodium in figures 9(a) and (b), respectively. AISI 316 stainless steel underwent immediate cavitation damage, as indicated by the macrograph for this material taken after 5 minutes of testing. After 4 hours of testing the cavitation damage to this specimen was quite severe. On the other hand, the Stellite 6B specimen still retained most of its original polish after 5 minutes of testing and even after 4 hours showed a relatively small amount of surface damage. Macrographs of specimens of all the alloys tested in sodium after 4 hours are shown in figure 10. The alloys can be arbitrarily separated into three groups, each displaying a different degree of cavitation damage:

- (1) Severe damage - annealed Sicromo 9M
- (2) Intermediate damage - AISI 316 and 318 stainless steels, Inconel 600, A-286, and Hastelloy X
- (3) Slight damage - L-605, René 41, and Stellite 6B

Although there are heavily damaged portions evident locally on the surfaces of the A-286 and L-605 specimens, these alloys have actually lost a smaller volume of material than AISI 318 stainless steel and Inconel 600, which are more uniformly damaged.

Macrographs of the materials after cavitation in mercury are shown in figure 11. Again, these materials can be separated by visual observation into three groups:

- (1) Severe damage - annealed Sicromo 9M and Hastelloy X
- (2) Intermediate damage - hardened Sicromo 9M and L-605
- (3) Slight damage - Stellite 6B

Comparison of figures 10 and 11 illustrates a marked difference between damage patterns caused by sodium and those caused by mercury. After testing in sodium, the specimen surface showed a damage pattern that was fine textured in appearance. The rims of the specimens were relatively undamaged. The mercury damage pattern, on the other hand, indicated a very coarse, deeply cratered surface. As indicated previously, these differences in surface appearance may be caused by different damage mechanisms, resulting from the widely different properties of the two fluids.

Photomicrographs of the same area on specimens tested in sodium for different times are shown in figure 12. At relatively high magnifications all specimens that were tested in sodium showed a nonuniform damage pattern. Three specific examples are shown in the figure. Type AISI 316 stainless steel showed severe matrix attack after only 5 minutes, while some grain and/or twin boundaries stood out in relief (fig. 12(a)). On the other hand, in L-605 both grain and twin boundaries were attacked more heavily than the matrix. This damage is evident after 45 minutes of testing (fig. 12(b)). Stellite 6B showed very slight matrix attack after 5 minutes. Only a few carbide particles were dislodged in the early phases of the test (fig. 12(c)). As test time was increased, more carbide particles were dislodged leaving deep pits. These pits, which widened with time, evidently served as sites for increased cavitation attack. It appears from these photomicrographs that although some of the carbide particles were dislodged, most of them remained intact, and their presence evidently is a major factor in making Stellite 6B highly resistant to cavitation damage.

In mercury, no particular portion of the microstructure of any of the materials except Stellite 6B appeared to be attacked preferentially. Alloy L-605 is typical of the materials showing a uniform damage pattern. Photomicrographs of this alloy after 1-minute exposure to cavitation in mercury are shown in figure 13(a). The preferential attack of Stellite 6B is illustrated in figure 13(b), which shows that the carbide particles are particularly resistant to cavitation attack; whereas, the softer matrix shows definite cavitation attack.

RELATION BETWEEN ACCELERATED CAVITATION DAMAGE AND MATERIAL PROPERTIES

It would obviously be useful to be able to predict which materials have superior resistance to cavitation damage from mechanical property data. Thus, a method of correlating cavitation damage with readily available material properties, even though empirical in nature, might serve as a guide to designers and as a substitute for accelerated cavitation tests.

One of the most recent attempts to achieve a method of ranking materials with respect to cavitation damage resistance in liquid metals (refs. 16 and 20) indicates that the severity of cavitation damage may be inversely related to the strain energy of materials. Strain energy is approximately equivalent to the area beneath the stress-strain curve and has been used as a measure of the toughness of a material. When the stress-strain curves are not available, strain energy can be approximated by the following equation (ref. 20):

$$S. E. = \left(\frac{Y. S. + T. S.}{2} \right) e \quad (1)$$

where

Y. S. yield strength

T. S. tensile strength

e elongation

The necessary properties for calculating the strain energy of materials at 800⁰ F are given in table V; figure 14 shows the relation between strain energy and the reciprocal of the steady-state volume loss rate of materials subjected to cavitation damage in sodium. The steady-state volume loss rate values were obtained from figure 6(a) at 4 hours. Although the volume loss rate curves indicate that Stellite 6B, and perhaps L-605, may not yet have reached a steady-state condition after 4 hours, the values for this test time were used as approximations of the steady-state rates.

It is evident from the figure that all the data do not fall close to a correlating line. The data point for the material that performed most favorably, Stellite 6B, is very far removed from the data of the other materials. Even if the steady-state damage rate of Stellite 6B should be higher than that assumed (as it may be with longer test time), it is quite certain that the reciprocal of the volume loss would not be displaced by the approximately one order of magnitude needed to make this data point fall into line. Thus, the use of this particular correlating parameter would have resulted in omitting from consideration one of the most favorable cavitation damage resistant materials.

It would seem that strain energy alone is not entirely representative of the properties that affect the resistance of a material to cavitation damage. The hardness, elastic modulus, and the fatigue limit are other readily measurable material properties that might be expected to have some effect on cavitation damage resistance. In order to evaluate their role adequately, extensive additional data (over a wide range of test conditions and with many materials) are needed. Finally, the validity of any such parameter would be affected by corrosion variables that differ for different environments and that might

in some cases be overriding. Thus, it is evident that additional research is needed to achieve a better understanding of the relations between cavitation damage and readily measurable material properties.

RELATION BETWEEN ACCELERATED CAVITATION DAMAGE AND PUMP IMPELLER TEST RESULTS

A qualitative comparison was made between the damage experienced by three materials, René 41 and AISI 316 and 318 stainless steels, tested in the accelerated cavitation damage facility and that experienced by the same materials when used as pump impeller vanes in sodium loop tests conducted at the Lewis Research Center (unpublished data from W. S. Cunnan, D. C. Reemsnyder, and C. Weigle). Visual observations indicated that the materials ranked in the same order with respect to resistance to cavitation damage after accelerated tests as after actual pump loop operation.

Macrographs of specimens subjected to accelerated cavitation damage are shown in figure 10. Macrographs of the damaged surfaces of impeller blades that were operated for 250 hours under cavitating conditions at temperatures up to 1500⁰ F are shown in figure 15. It is evident that the René 41 impeller showed virtually no cavitation damage; whereas, the AISI 318 and 316 stainless-steel blades had marked regions of damage. The degree of damage for the two stainless-steel blades was not appreciably different. When considered on a volume loss basis (fig. 5(a)), René 41 showed considerably less damage than either of these steels. Both steels, however, ranked very close together with respect to volume loss. It is significant that a qualitative agreement between the results of accelerated cavitation tests and full-scale impeller operation was obtained. Surface traces were taken of the damaged areas in an attempt to determine a quantitative measure of the cavitation damage; however, the extent of general corrosion of the blade surface masked the degree of localized cavitation damage. Although further verification is required for other materials, and under other operating conditions, these results suggest that the magnetostrictive accelerated cavitation test can provide a useful means of selecting materials suitable for longtime operation under cavitating conditions.

GENERAL REMARKS

Corrosion Effects

Previous investigations (refs. 7, 11, and 15) have indicated that corrosion can be a

contributing factor to cavitation damage. In pump impeller tests, blades tested for 250 hours under cavitating conditions in sodium showed corrosion over the entire blade surface as well as clearly delineated cavitation damaged areas (fig. 15). In the accelerated cavitation tests the contribution of corrosion to the total damage may be less than that normally found in longtime service under cavitating conditions. A possible way of determining the effect of corrosion in an accelerated cavitation test is to introduce hold times between periods of transducer excitation. This type of pulse test was used in an earlier investigation (ref. 11) to indicate the extent of corrosion damage associated with the cavitation process in aqueous solutions. Although the introduction of hold periods substantially lengthens the accelerated test, it may be a useful method of determining the additional contribution of corrosion to the total damage effect experienced by materials in accelerated liquid metal cavitation tests.

Oxygen Contamination in Sodium

Although reactor-grade sodium with very low initial oxygen content was used in this investigation, chemical analyses indicated that the oxygen level was near the limit of solubility after prolonged test times. In order to reduce the possibility of subjecting the individual materials to substantially different fluid environments, the various materials were tested concurrently. Each material was, in turn, subjected to cavitation damage for a short time, rather than conducting a complete test with one material before beginning a test with the next material. Also, fresh charges of sodium were introduced at several intervals. It was observed that the volume loss curves for individual materials did not show significant discontinuities when tests were resumed with the fresh charges of sodium.

Oxygen contamination is not considered to have particularly adverse effects on material properties of the steels and superalloys. It is important to note, however, that other materials, specifically the refractory metals, are adversely affected by exposure to oxygen in sodium at high temperatures. Columbium and tantalum, for example, are subject to severe embrittlement as a result of oxygen pickup. Furthermore, these metals are subject to accelerated corrosion attack when oxygen is present. Adequate measures must therefore be taken to avoid oxygen absorption when subjecting refractory metals to cavitation tests in sodium.

Selection of Materials for Use Under Cavitating Conditions

The materials considered in this investigation show wide differences in their resistance to cavitation damage. However, it is important to recognize that resistance to

cavitation damage is not the sole factor to be considered when selecting a material for use as a pump impeller in liquid metal systems. As in most engineering applications a compromise based on various material properties will probably be required. Thus, although Stellite 6B is far more resistant to cavitation damage than all the other materials considered, this alloy is notch sensitive and has relatively low ductility. In contrast, L-605, which has less resistance to cavitation damage, has greater ductility. This could be an overriding factor to a designer in choosing a material for pump impeller application in space power conversion systems. The preceding example, of course, illustrates only one other aspect besides resistance to cavitation damage, which must be investigated in making a material selection. Others, such as rupture strength, creep resistance, and stability on longtime exposure to elevated temperatures, must all be taken into consideration. The net result could well be that the order of resistance to cavitation damage would not necessarily be the order of choice of materials for pump impellers in space power systems.

SUMMARY OF RESULTS

start
The resistance to cavitation damage of candidate materials for components of liquid metal space power conversion systems was investigated in two liquid metal environments. A magnetostrictive apparatus was used to achieve an accelerated rate of cavitation damage. Tests were run in sodium at 800° F and in mercury at 300° F. The following results were obtained:

1. In all cases, the materials that were tested in both sodium and mercury ranked in the same order based on resistance to cavitation damage.
2. The severity of the cavitation damage experienced by all materials in mercury at 300° F was consistently greater than that experienced by the same materials in sodium at 800° F. For example, after 4 hours, the volume loss incurred by Stellite 6B and L-605 in mercury was approximately four to five times that encountered in sodium.
3. Stellite 6B was far superior to all other materials investigated. For example, in sodium when compared on a volume loss basis after 4 hours, the damage sustained by this alloy was approximately 15 percent of the volume-loss damage of L-605, one of the other more cavitation-resistant materials, and only 1 percent of the damage sustained by annealed Sicromo 9M, the most heavily damaged material. In mercury, the volume loss sustained by Stellite 6B was approximately 16 percent of that sustained by L-605 after 4 hours, and after 1 hour the volume loss of Stellite 6B was 2 percent that of annealed Sicromo 9M.
4. Surface roughness measurements provided a ranking of materials with respect to cavitation damage resistance similar to that obtained by conventional volume loss measurements.

5. Metallographic examination at high magnifications during the early stages of cavitation damage indicated that cavitation in sodium resulted in a nonuniform damage to all materials as evidenced by the delineation of twin and grain boundaries. Cavitation in mercury on the other hand resulted in a uniformly damaged surface with no apparent preferential attack except for Stellite 6B. In this alloy, the carbides were more resistant than the matrix. Examination at low magnifications after appreciable damage had occurred indicated that cavitation in sodium resulted in a fine-textured (matte) surface; whereas, exposure to mercury resulted in very coarse, deep craters.

6. Visual observations of pump impeller blades of AISI 316 and 318 stainless steels and René 41 tested under cavitating conditions for 250 hours at temperatures up to 1500⁰ F in sodium indicated the same ranking of these materials with regard to cavitation damage resistance as that determined in the accelerated tests of this investigation.

Lewis Research Center,
National Aeronautics and Space Administration,
Cleveland, Ohio, December 21, 1965.

end
///

REFERENCES

1. Kulp, Robert S.; and Altieri, James V.: Cavitation Damage of Mechanical Pump Impellers Operating in Liquid Metal Space Power Loops. Pratt and Whitney Aircraft (NASA CR-165), 1965.
2. Smith, P. G.; DeVan, J. H.; and Grindell, A. G.: Cavitation Damage to Centrifugal Pump Impellers During Operation with Liquid Metals and Molten Salt at 1050⁰ - 1400⁰ F. J. Basic Eng., vol. 85, no. 3, Sept. 1963, pp. 329-335; Discussion, pp. 335-337.
3. Smith, Willy; Nieto, Juan M.; and Hammitt, Frederick G.: Cavitation Damage Measurements in Mercury by Radiotracer Analysis. Rept. No. 03424-10-T, Mich. Univ. (NASA CR-53112), 1963.
4. Anon.: Sunflower Power Conversion System. Rept. No. ER-5163, Thompson Ramo Wooldridge, Inc. (NASA CR-56206), 1962.
5. Anon.: SNAP-8 Topical Materials Report for 1963. Vol. II - Development of Component Materials. Rep. No. 2822 (Special), Aerojet-General Corp., Mar. 1964.
6. Knapp, R. T.; and Hollander, A.: Laboratory Investigations of the Mechanism of Cavitation. Trans. ASME, vol. 70, no. 5, July 1948, pp. 419-431; Discussion, pp. 431-435.

7. Prieser, H. S. ; and Tytell, B. H. : The Electrochemical Approach to Cavitation Damage and its Prevention. *Corrosion*, vol. 17, no. 11, Nov. 1961, pp. 107-115; Discussion, pp. 115-121.
8. Knapp, Robert T. : Recent Investigations of the Mechanics of Cavitation and Cavitation Damage. *Trans. ASME*, vol. 77, no. 7, Oct. 1955, pp. 1045-1054.
9. Plesset, M. S. ; and Ellis, A. T. : On the Mechanism of Cavitation Damage. *Trans. ASME*, vol. 77, no. 7, Oct. 1955, pp. 1055-1064.
10. Naude, Charl F. ; and Ellis, Albert T. : On the Mechanism of Cavitation Damage by Non-Hemispherical Cavities Collapsing in Contact with a Solid Boundary. *J. Basic Eng.*, vol. 83, no. 4, Dec. 1961, pp. 648-656.
11. Plesset, Milton S. : Pulsing Technique for Studying Cavitation Erosion of Metals. *Corrosion*, vol. 18, no. 5, May 1962, pp. 181-188.
12. Wheeler, W. H. : Indentation of Metals by Cavitation. *J. Basic Eng.*, vol. 82, no. 1, Mar. 1960, pp. 184-191; Discussion, pp. 191-194.
13. Lichtman, J. Z. ; and Weingram, E. R. : Cavitation Design Handbook. Rep. No. NR 062-314, U. S. Naval Applied Science Lab., Brooklyn, New York, Sept. 30, 1964.
14. Hammitt, Frederick G. ; Robinson, M. John; Siebert, Clarence A. ; and Aydinmakine, Fazil A. : Cavitation Damage Correlations for Various Fluid-Material Combinations. Rept. No. 03424-14-T, Univ. Mich. (NASA CR-59666), 1964.
15. Leith, W. C. ; and Thompson, A. Lloyd: Some Corrosion Effects in Accelerated Cavitation Damage. *J. Basic Eng.*, vol. 82, no. 4, Dec. 1960, pp. 795-807.
16. Thiruvengadam, A. : A Unified Theory of Cavitation Damage. *J. Basic Eng.*, vol. 85, no. 3, Sept. 1963, pp. 365-376.
17. Hammitt, F. G. ; Chu, P. T. ; Ivany, R. D. ; Robinson, M. J. ; Biss, V. ; Cramer, V. F. ; Pehlke, R. D. ; and Siebert, C. A. : Cavitation Damage Tests with Water in a Cavitating Venturi. Tech. Rept. No. 03424-4-T. Department of Nuclear Engineering, College of Engineering, Univ. of Michigan, Mar. 1962.
18. Prieser, H. S. ; Thiruvengadam, A. ; and Couchman, C. : Cavitation Damage Research Facilities for High Temperature Liquid Alkali Metal Studies. Symposium on Cavitation Research Facilities and Techniques, J. William Holl and Glenn M. Wood, eds., ASME, 1964, pp. 146-156.

19. Kelly, R. W. ; Wood, G. M. ; Marman, H. V. ; and Milich, J. J. : Rotating Disk Approach for Cavitation Damage Studies in High Temperature Liquid Metal. Paper No. 63-AHGT-26, ASME, Mar. 1963.
20. Thiruvengadam, A. ; Couchman, C. , III; and Preiser, H. S. : Cavitation Damage Resistance of Materials in Liquid Sodium. Paper 64-363, AIAA, June-July, 1964.
21. Anon. : Wear Resistant Alloys. Bulletin no. F30-1-33-A, Haynes Stellite Co. , 1962.
22. AMS Specifications: Rene 41-AMS5712; L605-AMS5759B; Hastelloy X - AMS5754D; A286-AMS5736B; Inconel-AMS5665G; and Type 316 Stainless Steel - AMS5648C.
23. Anon. : Stainless Steel Handbook. Allegheny Ludlum Steel Corp. , 1951.
24. Anon. : High Alloy Castings. Bulletin no. 261, Duraloy Co. , 1961.
25. Weiss, V. ; and Sessler, J. G. , eds. : Aerospace Structural Metals Handbook, Syracuse University Press, 1963.

TABLE I. - NOMINAL CHEMICAL COMPOSITIONS OF TEST MATERIALS

Material	Composition, weight percent														
	Iron	Nickel	Cobalt	Chromium	Molybdenum	Tungsten	Columbium	Titanium	Aluminum	Carbon	Manganese	Silicon	Phosphorous	Sulfur	Other
Stellite 6B (ref. 21)	a ₃	a ₃	Bal.	30	a _{1.5}	4.5	---	---	---	1.1	a ₂	a ₂	---	---	---
René 41 (AMS 5712, ref. 22)	a ₅	Bal.	10 to 12	18 to 20	9 to 10.5	---	---	3 to 3.3	1.4 to 1.8	a _{0.12}	a _{0.10}	a _{0.50}	---	a _{0.015}	0.003 to 0.01 (boron)
L-605 (AMS 5759 B, ref. 22)	a ₃	9 to 11	Bal.	19 to 21	---	14 to 16	---	---	---	0.05 to 0.15	1 to 2	a _{1.0}	a _{0.04}	a _{0.03}	---
Hastelloy X (AMS 5754 D, ref. 22)	17 to 20	Bal.	0.5 to 2.5	20.5 to 23	8 to 10	0.2 to 1.0	---	---	---	0.05 to 0.15	a _{1.0}	a _{1.0}	a _{0.04}	a _{0.03}	---
A-286 (AMS 5736 B, ref. 22)	Bal.	24 to 27	---	13.5 to 16	1 to 1.5	---	---	1.9 to 2.3	a _{0.35}	a _{0.08}	1 to 2	0.4 to 1	0.04	0.03	0.003 to 0.01 (boron) 0.1 to 0.5 (vanadium)
Inconel 600 (AMS 5665 G, ref. 22)	6 to 10	Bal.	a ₁	14 to 17	---	---	a ₁	a _{0.5}	a _{0.35}	a _{0.15}	a _{1.0}	a _{0.5}	---	a _{0.015}	a _{0.5} (copper)
AISI 318 stainless steel (ref. 23)	Bal.	13 to 15	---	17 to 19	2 to 2.75	---	0.8 (min)	---	---	a _{0.08}	a _{2.5}	a _{1.0}	---	---	---
AISI 316 stainless steel (AMS 5648 C, ref. 22)	Bal.	12 to 14	---	17 to 19	2 to 3	---	---	---	---	0.08	1.25 to a _{2.0}	a _{1.0}	a _{0.04}	a _{0.03}	a _{0.50} (copper)
Sicrom 9M (ref. 24)	Bal.	---	---	8 to 10	0.9 to 1.2	---	---	---	---	a _{0.2}	0.35 to 0.65	a _{1.0}	a _{0.04}	a _{0.04}	---

^aMaximum.

TABLE II. - HEAT TREATMENTS AND DENSITIES

OF TEST MATERIALS

Material	Heat treatment	Density, g/cm ³
Stellite 6B	Solution-heat treated at 2250° F; air cooled	8.38
René 41	Solution-heat treated at 1975° F; rapid quenched	8.25
L-605	Solution-heat treated at 2250° F; water quenched	9.13
Hastelloy X	Solution-heat treated at 2150° F; rapid air cooled	8.23
A-286	Solution-heat treated at 1800° F; water quenched; aged at 1325° F for 16 hr	7.94
Inconel 600	Annealed	8.43
AISI 318 stainless steel	Annealed	7.99
AISI 316 stainless steel	Annealed	7.98
Sicromo 9M	Annealed; heat treated at 1750° F for 1 hr, then at 1350° F for 1 hr; air cooled	7.61

TABLE III. - CAVITATION TEST RESULTS

(a) Sodium at 800° F

Material	Volume loss, ^a mm ³				Steady-state volume loss rate, mm ³ /hr	Surface roughness, ^a μ in.			
	Time, hr					Time, hr			
	1	2	3	4		1	2	3	4
Stellite 6B	-----	0.04	0.13	0.39	^b 0.4	---	---	---	50
René 41	-----	.20	1.12	2.42	^b 1.3	15	40	65	85
L-605	-----	.22	1.25	2.58	^b 1.4	35	55	75	100
Hastelloy X	0.66	3.10	5.78	8.14	2.4	---	---	---	---
A-286	1.40	4.70	7.67	10.4	2.8	---	---	---	---
Inconel 600	2.70	6.40	10.3	13.4	3.1	---	---	---	---
AISI 318 stainless steel	2.90	7.16	11.8	15.9	4.1	80	100	115	120
AISI 316 stainless steel	3.64	8.63	13.8	18.0	4.2	---	---	---	---
Annealed Sicromo 9M	6.40	15.5	24.7	33.9	9.2	235	290	320	335

(b) Mercury at 300° F

Stellite 6B	0.34	0.75	1.28	1.81	^b 0.6	65	100	125	150
Hardened Sicromo 9M	1.07	3.45	6.80	10.5	3.4	155	260	450	700
L-605	1.12	4.00	7.60	11.3	3.6	265	365	525	750
Hastelloy X	5.02	-----	-----	-----	^b 8.2	510	---	---	---
Annealed Sicromo 9M	18.2	-----	-----	-----	17.4	765	---	---	---

^aValues taken from curves faired through actual data.^bMay not have reached steady state.

TABLE IV. - TYPICAL SURFACE ROUGHNESS TRACES COMPARED WITH
VOLUME LOSS MEASUREMENTS FOR L-605 IN MERCURY AT 300° F

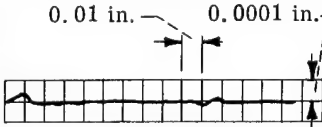
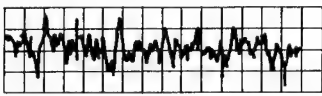
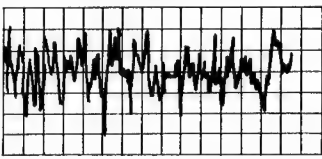
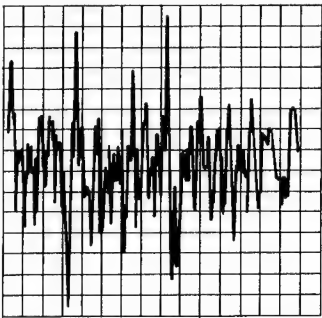
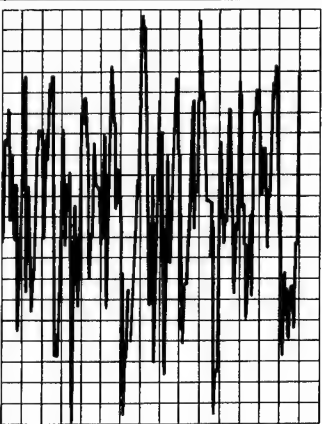
Time, min.	Volume loss, mm ³	Arithmetic average surface roughness, μ in.	Surface roughness trace
0	-----	<5	
1	<0.01	30	
4	0.05	50	
16	0.15	110	
60	1.12	260	

TABLE V. - MATERIAL PROPERTIES AT 800° F AND CALCULATED
STRAIN ENERGY PARAMETER FOR SODIUM TESTS

Material	Ultimate tensile strength, psi	Yield strength (0.2 percent offset), psi	Elongation, percent	Calculated strain energy, ^a kg/mm ²
Stellite 6B (ref. 21)	138 000	71 000	29.0	21.3
L-605 (ref. 25)	119 000	35 000	75.0	40.6
Hastelloy X (ref. 25)	100 000	47 000	50.0	25.8
A-286 (ref. 25)	137 000	92 000	21.0	16.9
Inconel 600 (ref. 25)	88 000	29 000	49.0	20.1
AISI 316 stainless steel (ref. 25)	70 000	28 000	40.0	13.8

^aStrain energy = $\left(\frac{\text{yield strength} + \text{tensile strength}}{2} \right) \times \text{elongation}.$

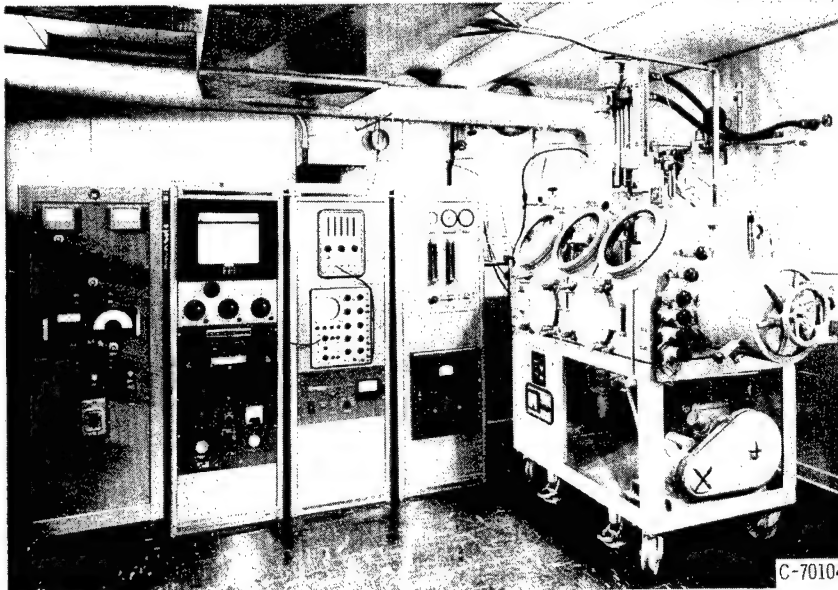


Figure 1. - Cavitation test facility.

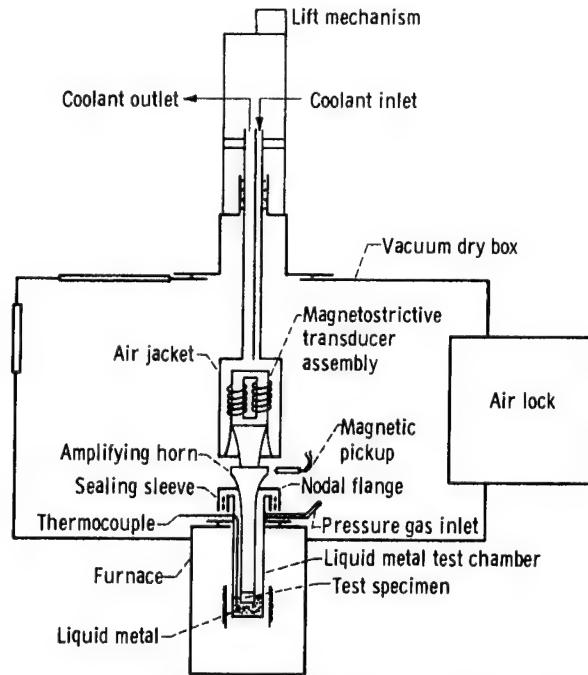


Figure 2. - Schematic diagram of magnetostrictive cavitation apparatus.

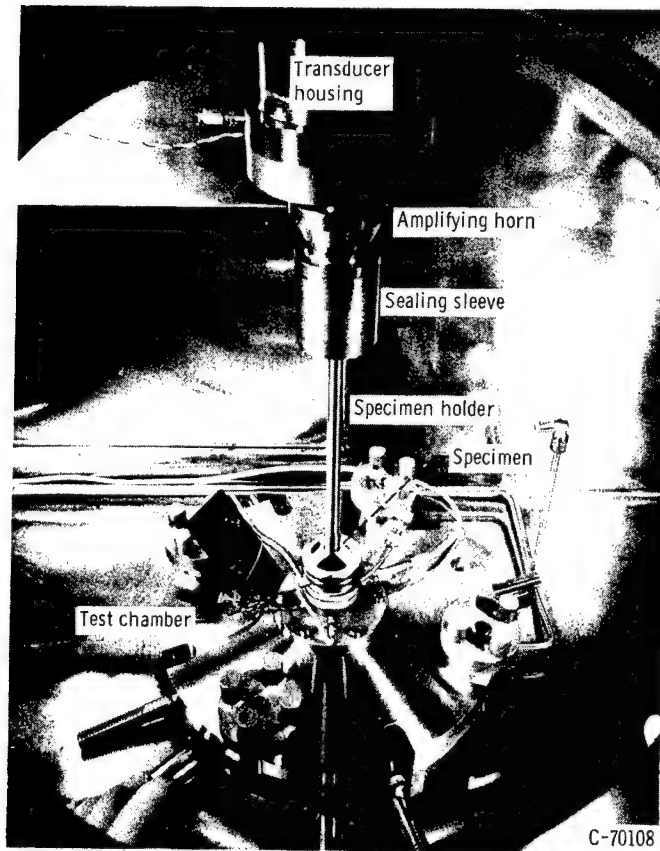


Figure 3. - Components of transducer assembly and liquid metal test chamber.

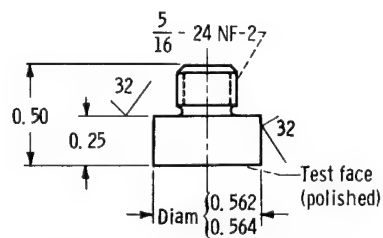


Figure 4 - Cavitation test specimen.

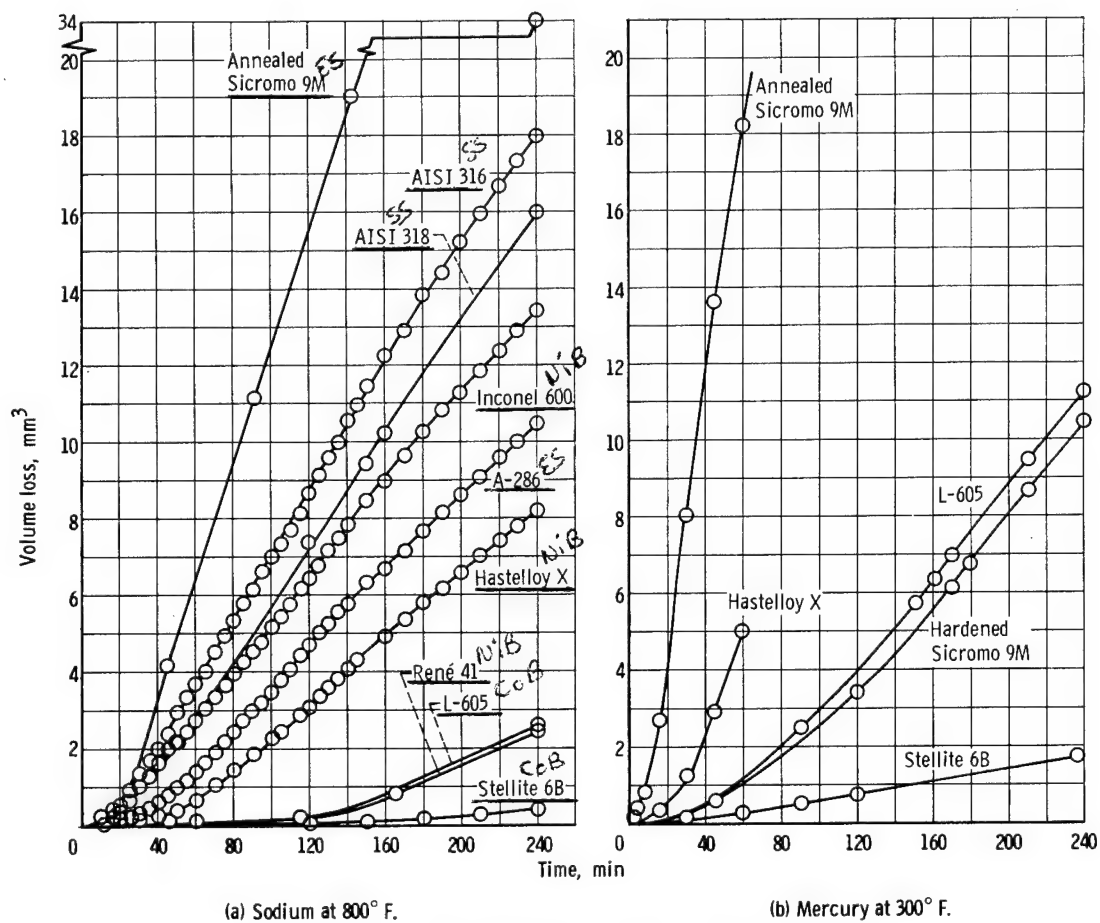
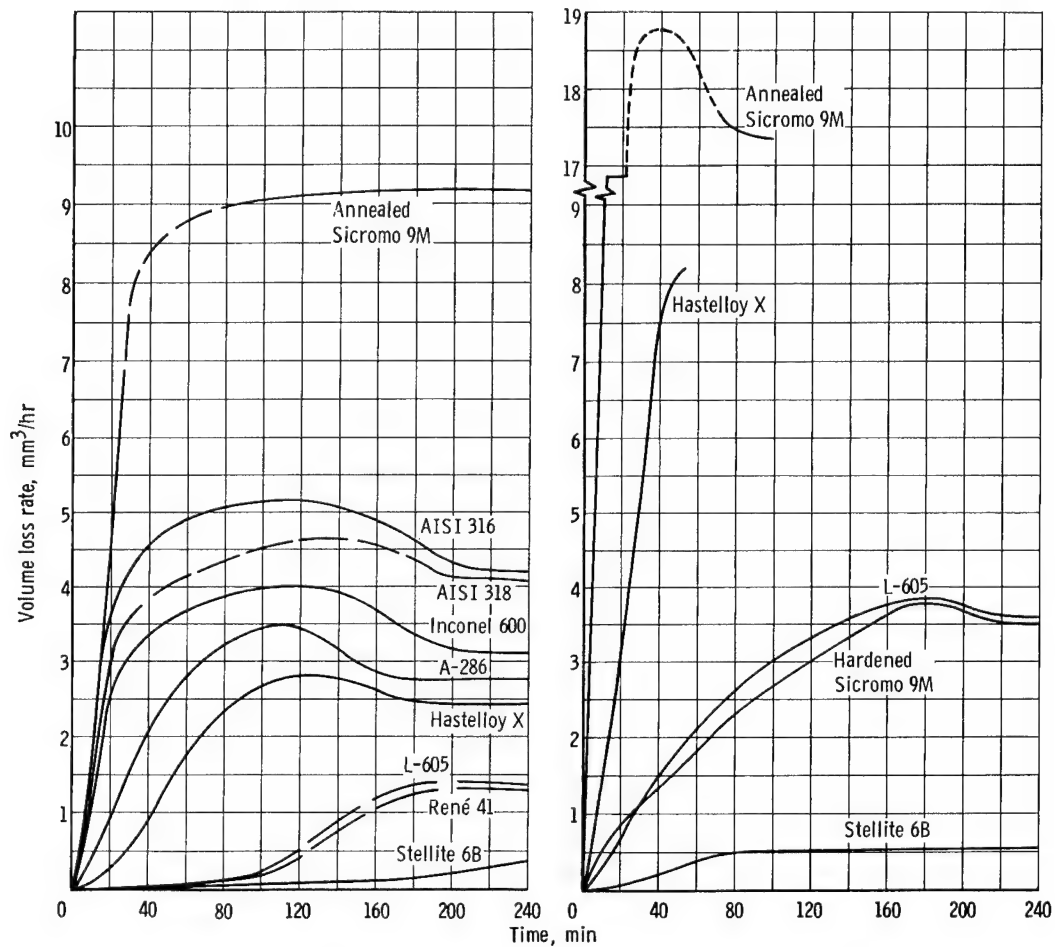


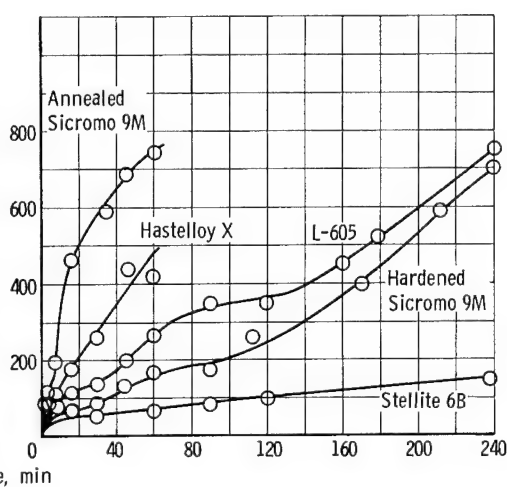
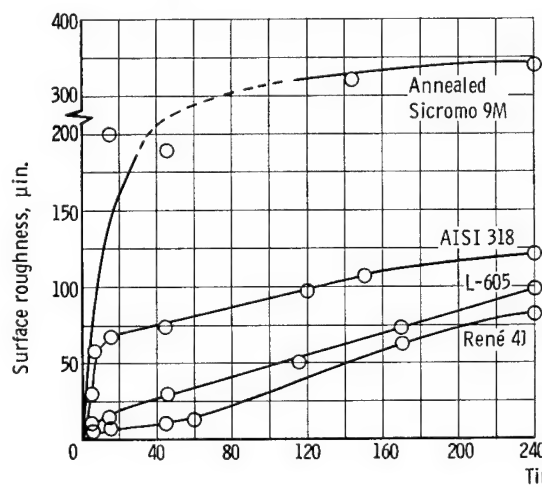
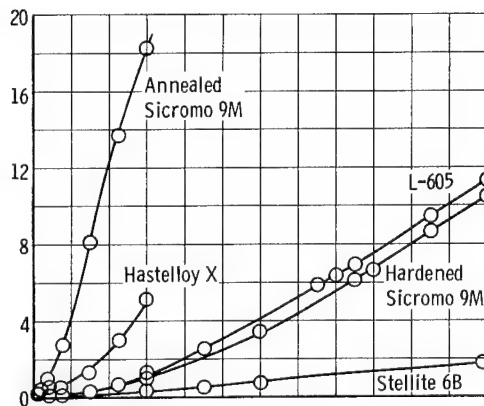
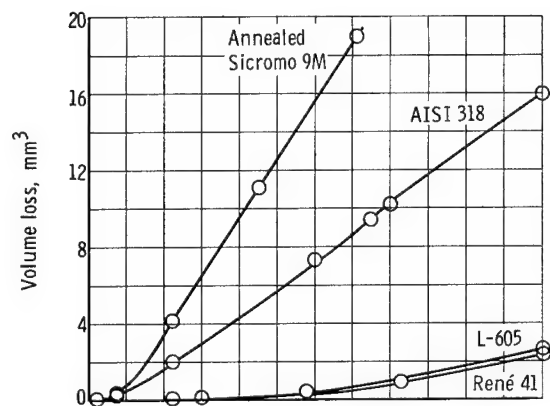
Figure 5 - Cavitation damage of materials in liquid metals.



(a) Sodium at 800°F .

(b) Mercury at 300°F .

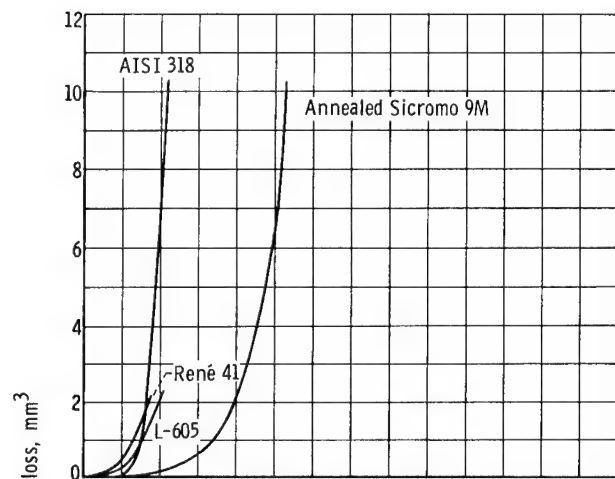
Figure 6. - Rate of cavitation damage of materials in liquid metals.



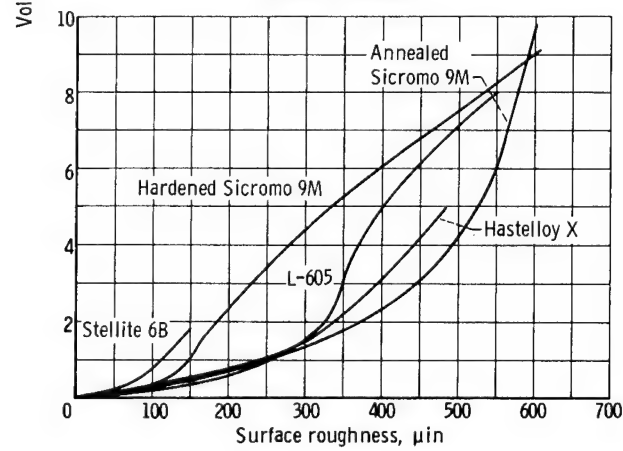
(a) Sodium at 800° F.

(b) Mercury at 300° F.

Figure 7. - Comparison of surface roughness and volume loss for alloys exposed to cavitation in liquid metals.

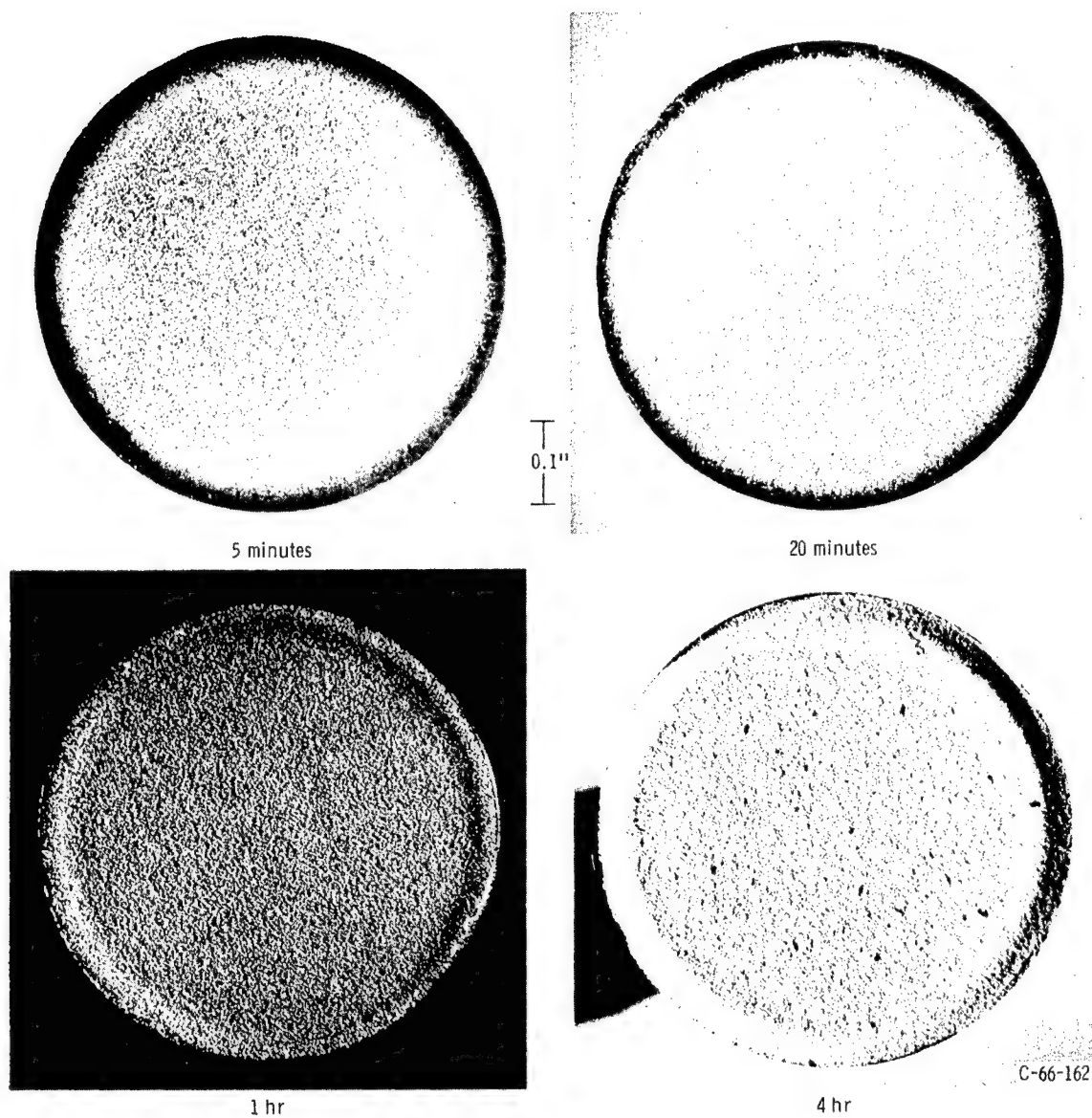


(a) Sodium at 800° F.



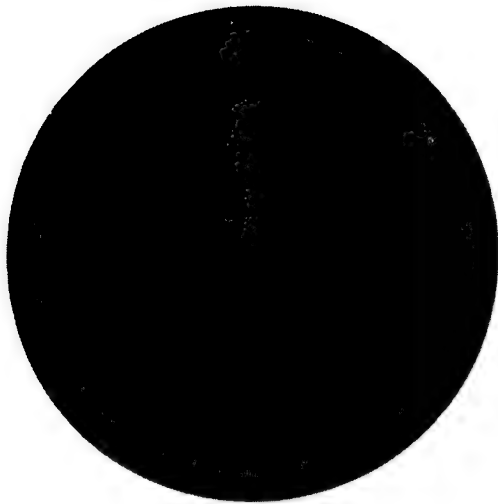
(b) Mercury at 300° F.

Figure 8 - Relation between volume loss and surface roughness.



(a) AISI 316 stainless steel.

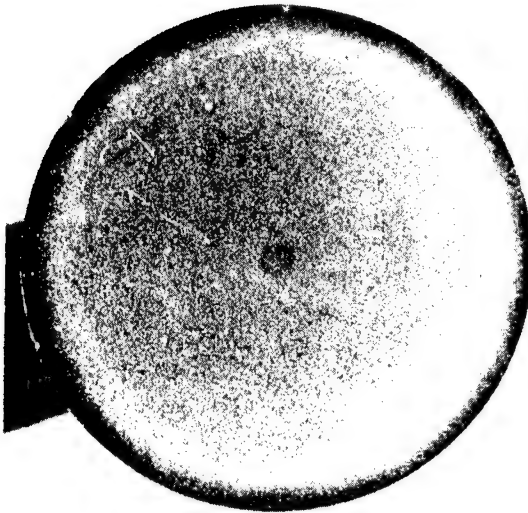
Figure 9. - Damaged surfaces of specimens after exposure to cavitation in sodium at 800° F.



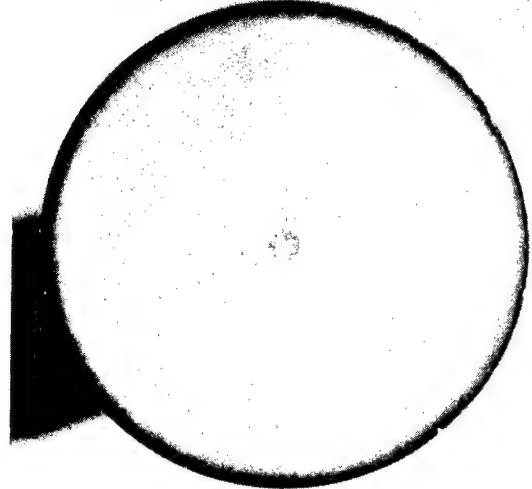
5 minutes



20 minutes



1 hr



4 hr

C-66-163

(b) Stellite 6B.

Figure 9. - Concluded.

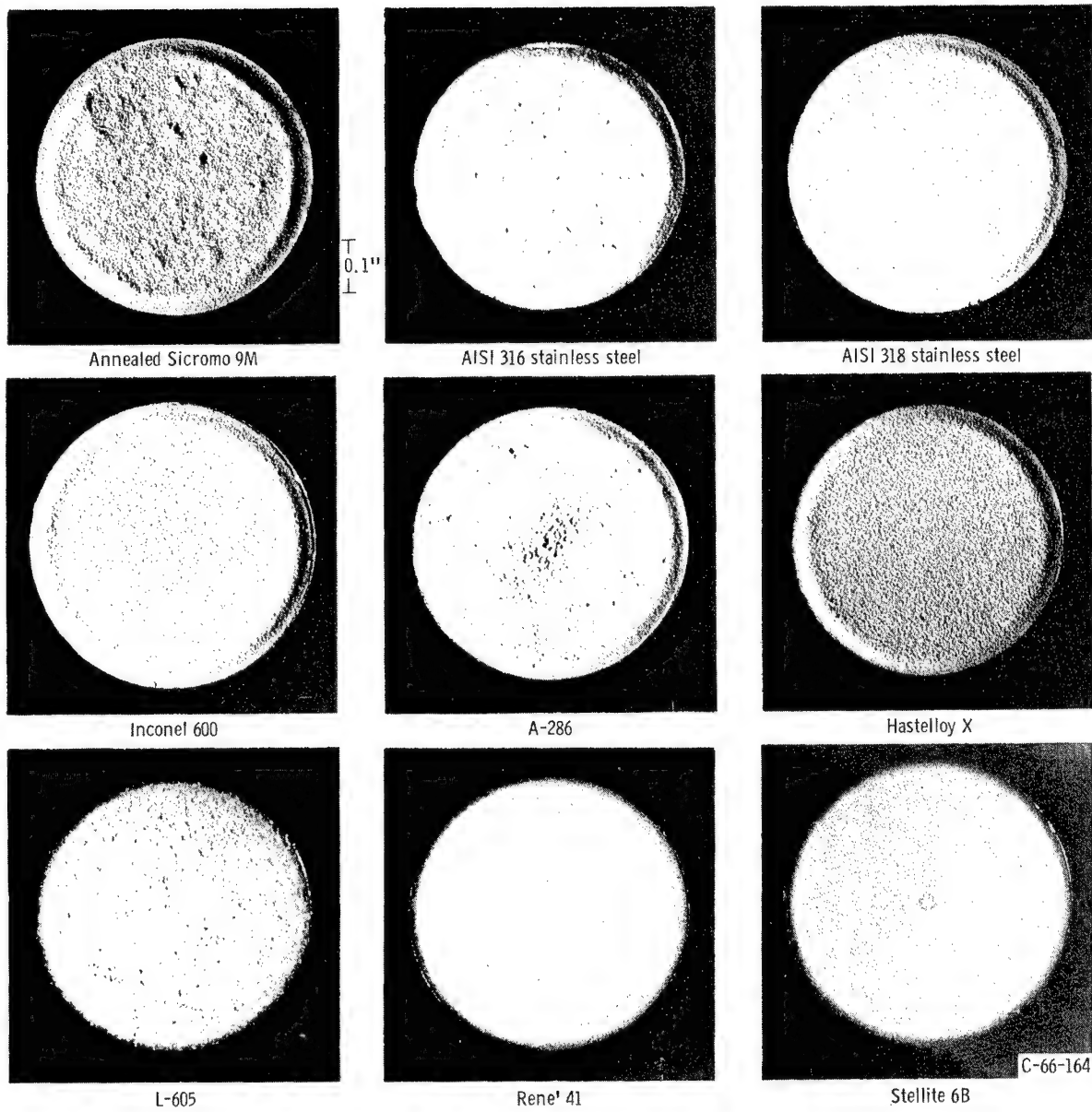


Figure 10. - Damaged surfaces of specimens after exposure to cavitation in sodium at 800° F for 4 hours.

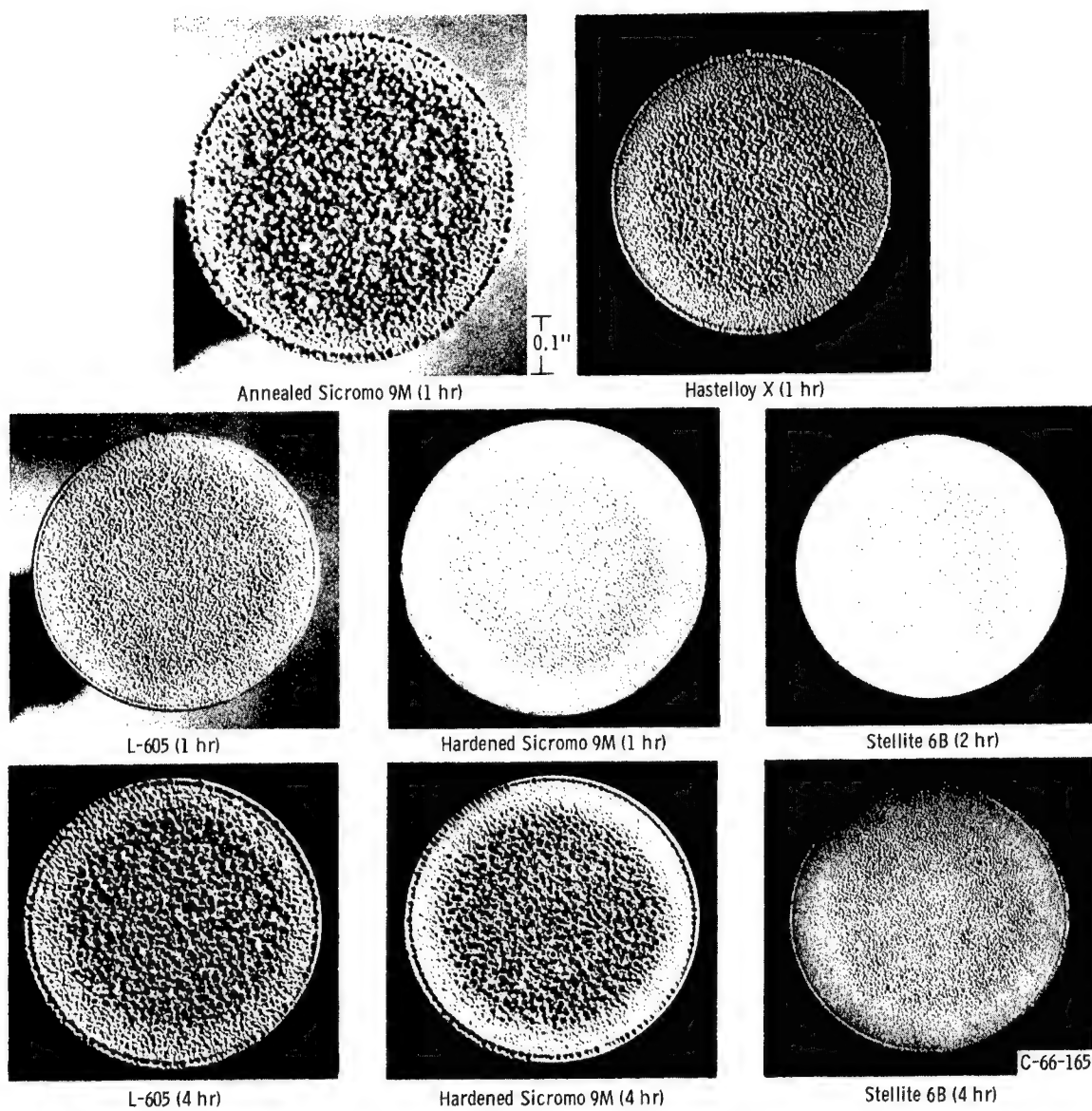


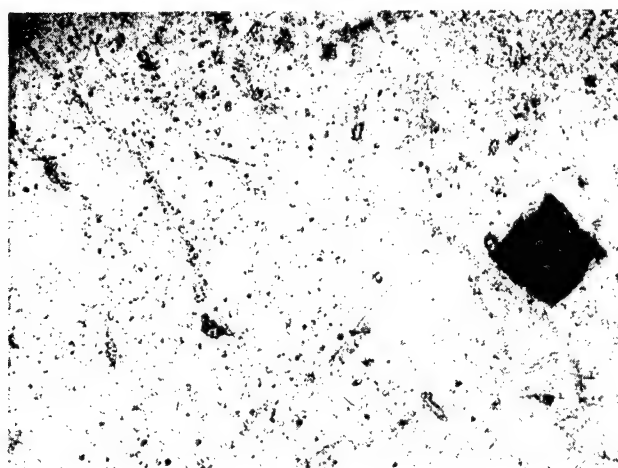
Figure 11. - Damaged surfaces of specimens after exposure to cavitation in mercury at 300° F.



Figure 12. - Photomicrographs of damaged surfaces of specimens exposed to cavitation in sodium at 800° F. X250.



0 min



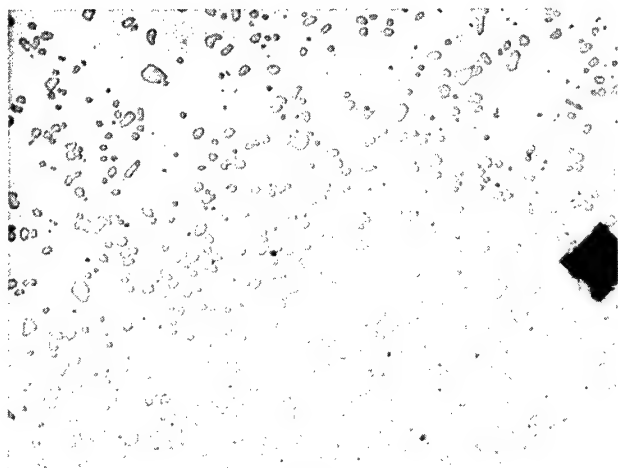
5 min



45 min

(b) L-605. (Reduced 30 percent in printing.)

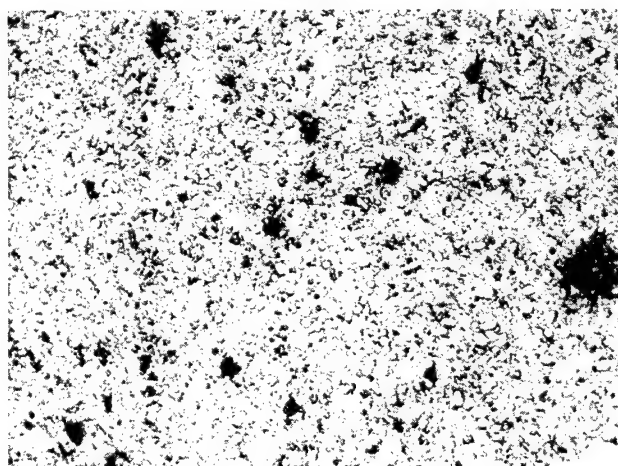
Figure 12. - Continued.



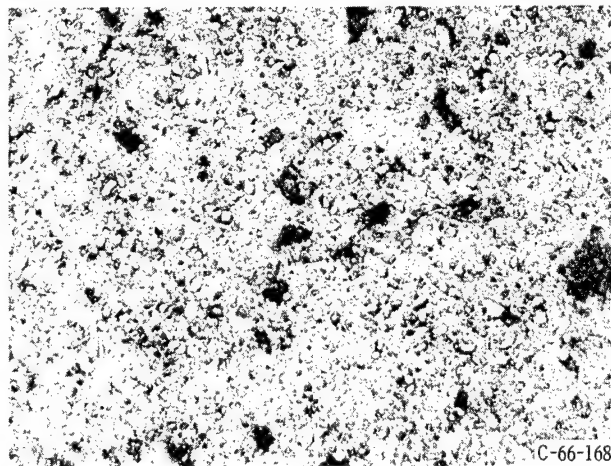
0 min



5 min



60 min

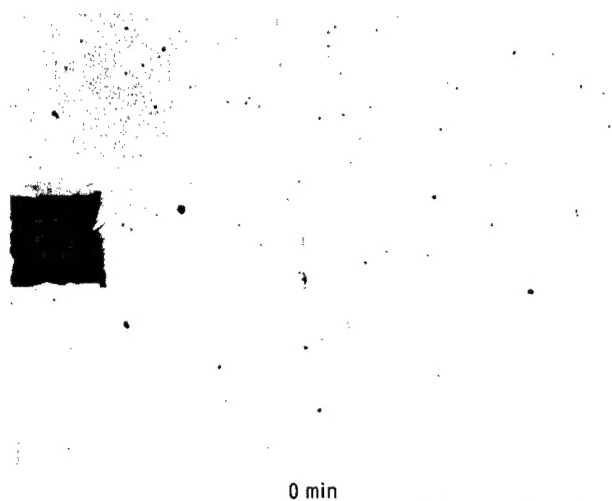


90 min

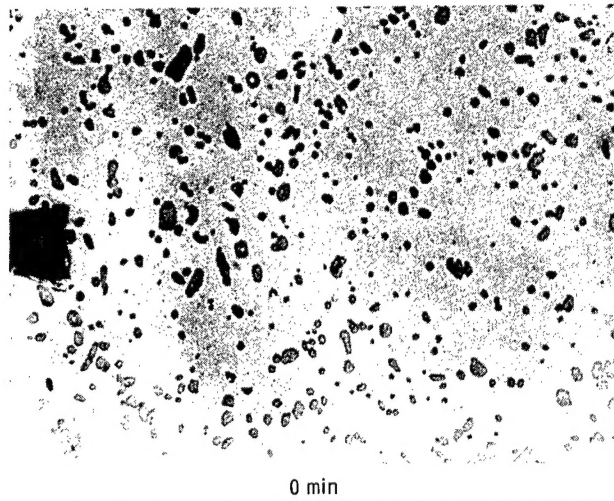
C-66-168

(c) Stellite 6B. (Reduced 30 percent in printing.)

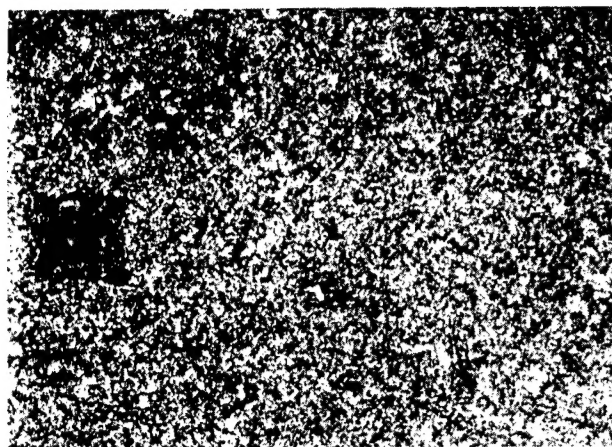
Figure 12. - Concluded.



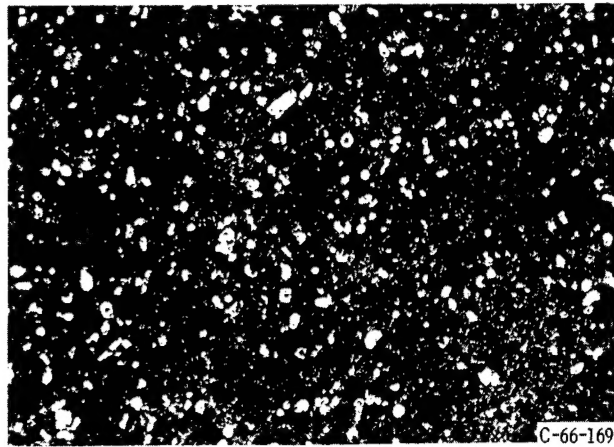
0 min



0 min



1 min
(a) L-605.



2 min
(b) Stellite 6B.

Figure 13. - Photomicrographs of damaged surfaces of specimens exposed to cavitation in mercury at 300° F. X250. (Reduced 30 percent in printing.)

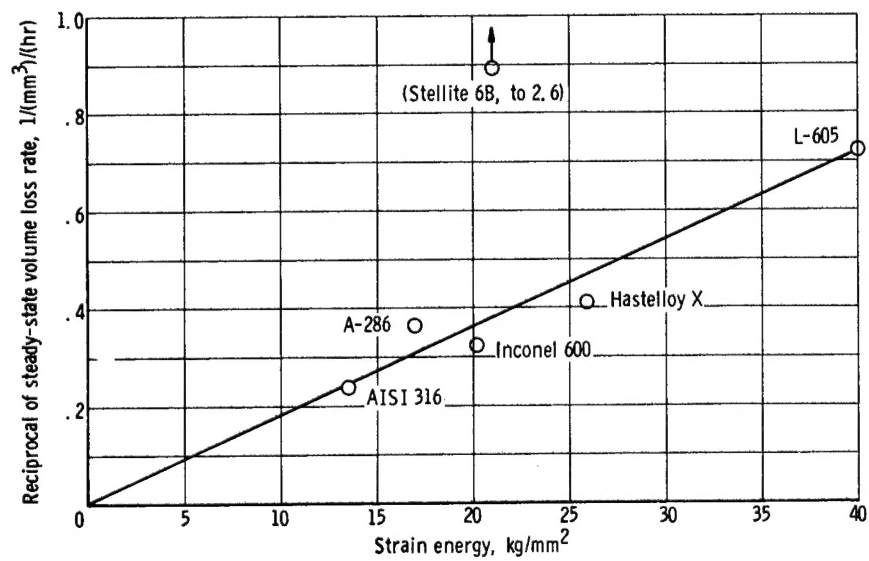


Figure 14. - Relation of cavitation damage in sodium with strain energy parameter.

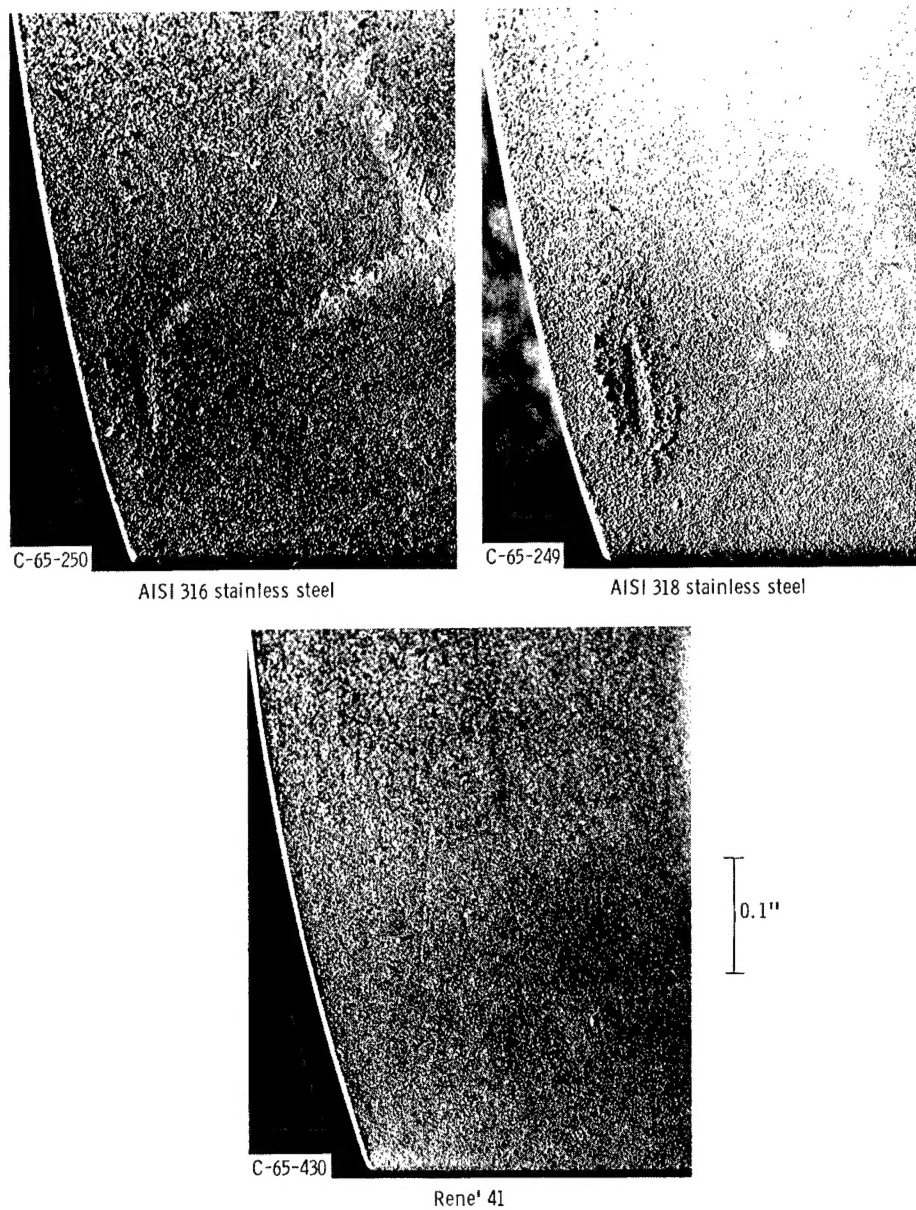


Figure 15. - Cavitation damage to pump impeller blades operated in liquid sodium for 250 hours up to 1500° F.

"The aeronautical and space activities of the United States shall be conducted so as to contribute . . . to the expansion of human knowledge of phenomena in the atmosphere and space. The Administration shall provide for the widest practicable and appropriate dissemination of information concerning its activities and the results thereof."

—NATIONAL AERONAUTICS AND SPACE ACT OF 1958

NASA SCIENTIFIC AND TECHNICAL PUBLICATIONS

TECHNICAL REPORTS: Scientific and technical information considered important, complete, and a lasting contribution to existing knowledge.

TECHNICAL NOTES: Information less broad in scope but nevertheless of importance as a contribution to existing knowledge.

TECHNICAL MEMORANDUMS: Information receiving limited distribution because of preliminary data, security classification, or other reasons.

CONTRACTOR REPORTS: Technical information generated in connection with a NASA contract or grant and released under NASA auspices.

TECHNICAL TRANSLATIONS: Information published in a foreign language considered to merit NASA distribution in English.

TECHNICAL REPRINTS: Information derived from NASA activities and initially published in the form of journal articles.

SPECIAL PUBLICATIONS: Information derived from or of value to NASA activities but not necessarily reporting the results of individual NASA-programmed scientific efforts. Publications include conference proceedings, monographs, data compilations, handbooks, sourcebooks, and special bibliographies.

Details on the availability of these publications may be obtained from:

SCIENTIFIC AND TECHNICAL INFORMATION DIVISION
NATIONAL AERONAUTICS AND SPACE ADMINISTRATION
Washington, D.C. 20546